



Heavy quark interaction in hot QCD matter: open charm and bottom dynamics in relativistic heavy-ion collisions

Maria Lucia Sambataro

In collaboration with: V. Minissale, S. Plumari, V. Greco

Dipartimento di Fisica e Astronomia 'E.Majorana'- Università degli Studi di Catania

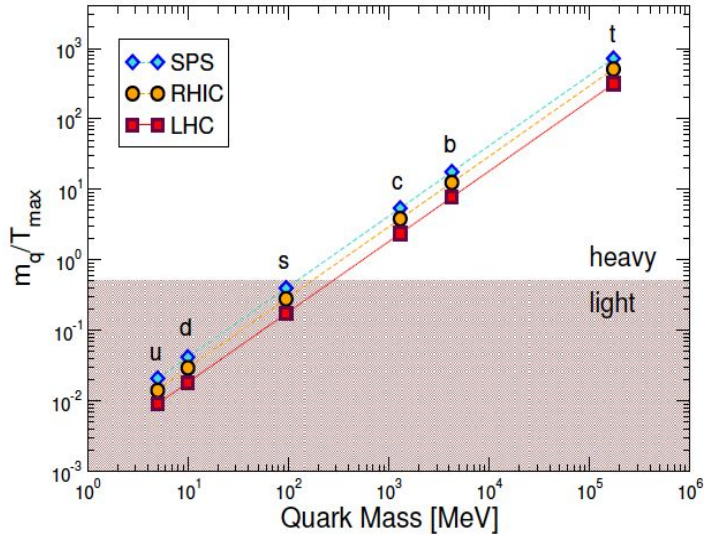
INFN -Laboratori Nazionali del Sud (LNS)

Outline

- **Catania Quasi-Particle Model for charm quark dynamics:**
 R_{AA} , v_n and their correlations \rightarrow Spatial diffusion coefficient D_s (T) of charm.
- **Predictions for bottom quark**
 R_{AA} , v_2 and v_3 of electrons from semileptonic B-meson decay.
- **Spatial diffusion coefficient D_s (T): charm vs bottom and the infinite mass limit**
- **Preliminary:** Extension to momentum dependent QPM
- Conclusions and new perspectives

Basic scales of charm and bottom quarks

Charm $M_c \approx 1.3$ GeV and Bottom $M_b \approx 4.2$ GeV



- $m_{c,b} \gg \Lambda_{QCD}$
pQCD initial production
- $m_{c,b} \gg T_{RHIC,LHC}$
negligible thermal production
- $\tau_0 < 0,08$ fm/c $\ll \tau_{QGP}$
- $\tau_{th} \approx \tau_{QGP} \gg \tau_{g,q}$

They experience the full evolution of the QGP.

They carry more informations with respect to their light counterparts.

Initial
production

$\tau_0 < 0.1$ fm/c

Dynamics in
QGP

B, D, Λ_c

b, c

b, c

B, D, Λ_c

Adapted from
Rapp & Greco

Hadronization:
Final hadron
Spectra and
observables

Reviews:

1. X.Dong, V. Greco Prog. Part. Nucl. Phys. 104 (2019),
2. A.Andronic EPJ C76 (2016), 3) R.Rapp, F.Prino J.Phys. G43 (2016)

CATANIA MODEL: QUASI-PARTICLE MODEL AND TRANSPORT THEORY

R_{AA}, v_n and $v_n - v_m$ correlations
in charm sector

Quasi Particle Model (QPM) fitting IQCD

Non perturbative dynamics \rightarrow M scattering matrices (q,g \rightarrow Q)
evaluated by Quasi-Particle Model fit to **IQCD thermodynamics**

$N_f=2+1$
Bulk:
u,d,s

$$m_g^2(T) = \frac{2N_c}{N_c^2 - 1} g^2(T) T^2$$

$$m_q^2(T) = \frac{1}{N_c} g^2(T) T^2$$



**Thermal masses of gluons
and light quarks**

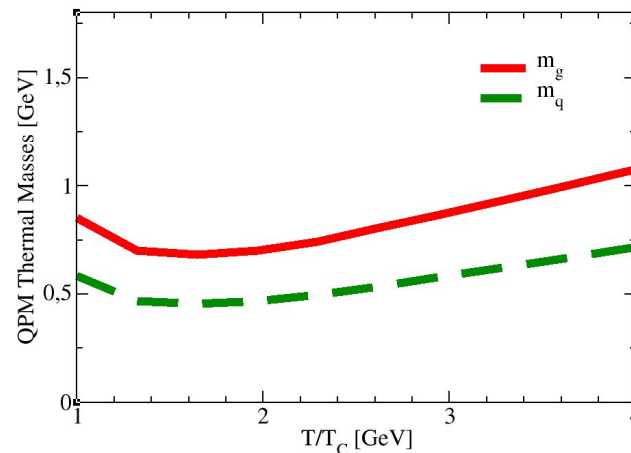
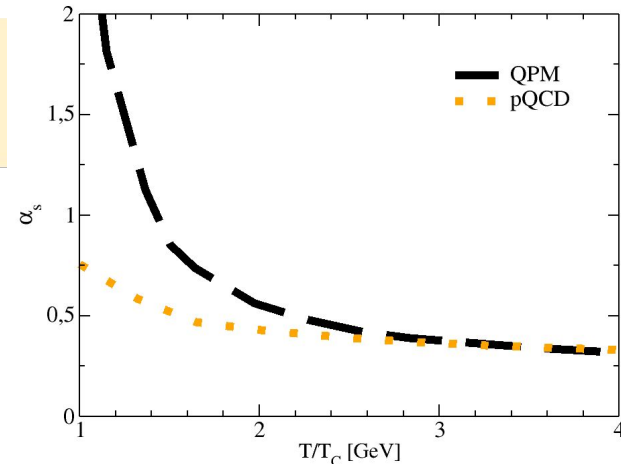
$g(T)$ from a fit to ϵ from IQCD data \rightarrow good reproduction of P, ϵ -3P

$$g^2(T) = \frac{48\pi^2}{(11N_c - 2N_f) \ln \left[\lambda \left(\frac{T}{T_c} - \frac{T_s}{T_c} \right) \right]^2}$$

$$\lambda=2.6$$

$$T_s=0.57 T_c$$

Larger than pQCD especially as $T \rightarrow T_c$



Relativistic Boltzmann equation at finite η/s

Bulk evolution

$$p^\mu \partial_\mu f_q(x, p) + m(x) \partial_\mu^x m(x) \partial_p^\mu f_q(x, p) = C[f_q, f_g]$$

$$p^\mu \partial_\mu f_g(x, p) + m(x) \partial_\mu^x m(x) \partial_p^\mu f_g(x, p) = C[f_q, f_g]$$

Free-streaming

field interaction

$$\varepsilon - 3p \neq 0$$

Collision term

gauged to some $\eta/s \neq 0$

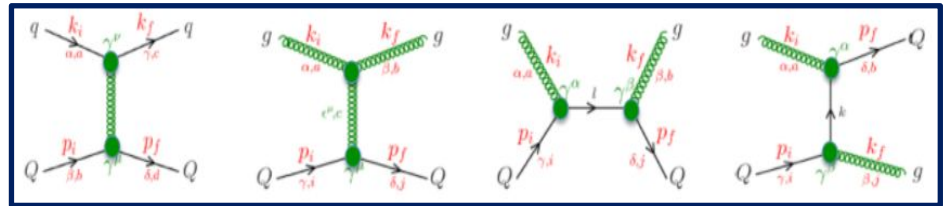
Equivalent to
viscous hydro at $\eta/s \approx 0.1$

HQ evolution

$$p^\mu \partial_\mu f_Q(x, p) = C[f_q, f_g, f_Q]$$

$$C[f_q, f_g, f_Q] = \frac{1}{2E_1} \int \frac{d^3 p_2}{2E_2 (2\pi)^3} \int \frac{d^3 p_1'}{2E_1' (2\pi)^3} \\ \times [f_Q(p_1') f_{q,g}(p_2') - f_Q(p_1) f_{q,g}(p_2)] \\ \times |M_{(q,g) \rightarrow Q}(p_1 p_2 \rightarrow p_1' p_2')| \\ \times (2\pi)^4 \delta^4(p_1 + p_2 - p_1' - p_2')$$

Feynman diagrams at first order pQCD for HQs-bulk interaction:

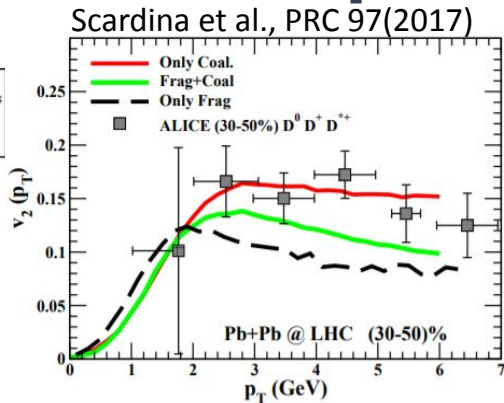
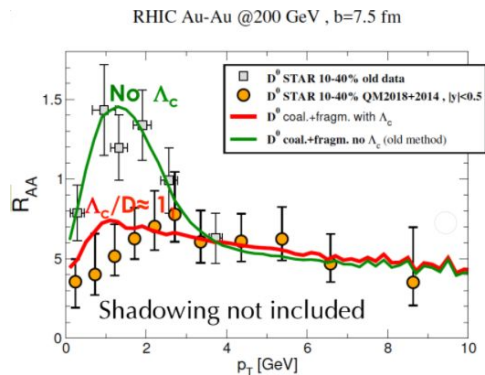


Scattering matrices $M_{g,q}$ by QPM fit to IQCD thermodynamics

HADRONIZATION: hybrid Coalescence + fragmentation

For details: S. Plumari talk [29 Sept at 11.15]

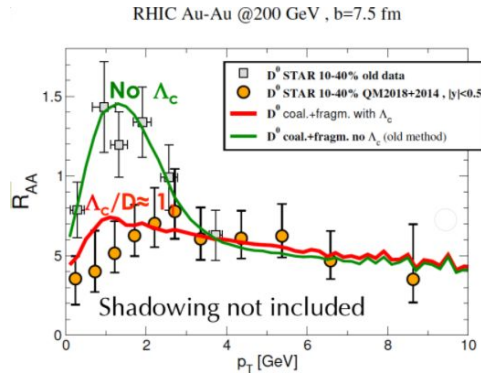
Catania QPM: some prediction for charm...



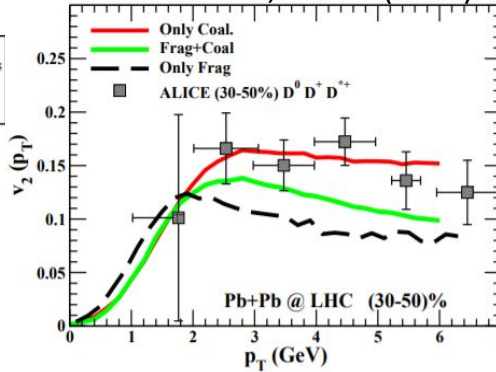
Good description of

R_{AA}, v_2 at RHIC & LHC energies
within error bars

Catania QPM: some prediction for charm...



Scardina et al., PRC 97(2017)

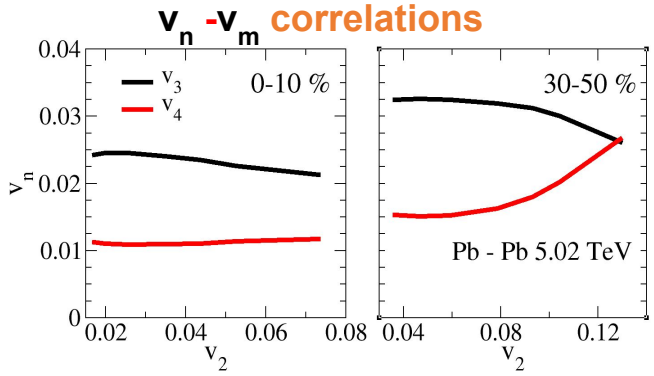


Good description of R_{AA}, v_2 at RHIC & LHC energies within error bars

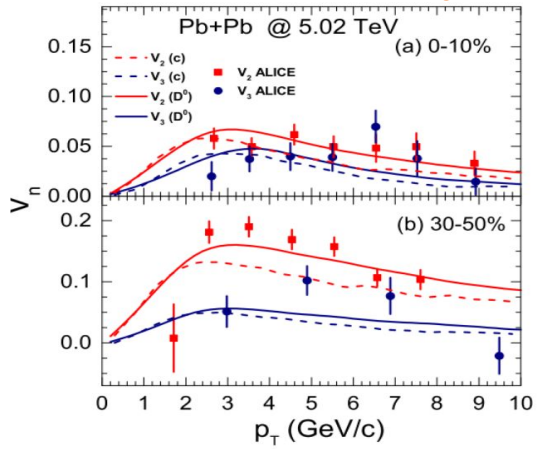
Monte Carlo Glauber for initial condition of partons
S.Plumari et al, *Phys.Rev.C* 92 (2015) 5

Predictions for D mesons

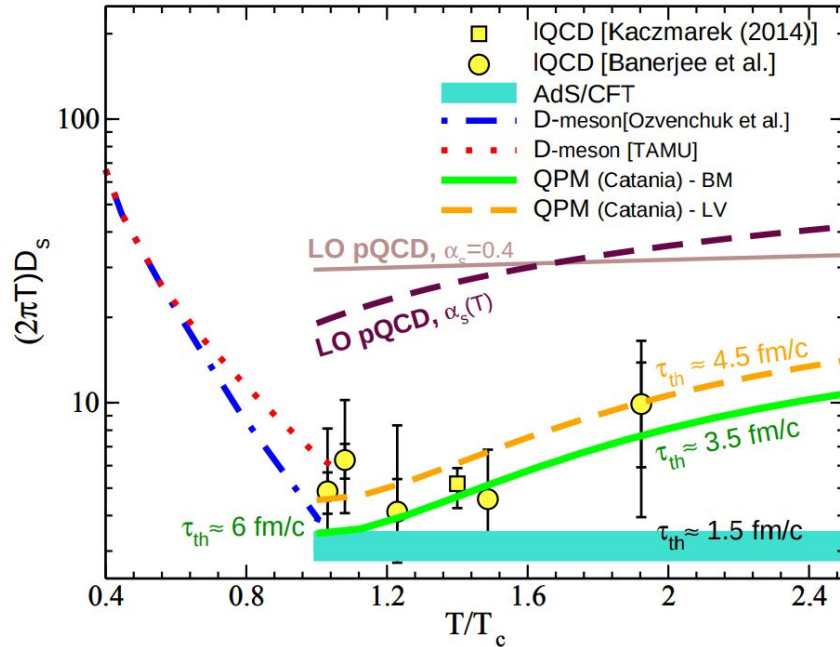
- Event-Shape Engineering Technique: Prediction for similar correlation for hard particles wrt bulk



Triangular flow v_3



Spatial diffusion coefficient of charm quark



Not a model fit to IQCD data, but D_s estimate that comes from results of $R_{AA}(p_T)$ and $v_2(p_T)$

We have a probe with $\tau_{therm} \approx \tau_{QGP}$

$$\tau_{th} = \frac{M}{2\pi T^2} (2\pi T D_s) \cong 1.8 \frac{2\pi T D_s}{(T/T_c)^2} \text{ fm/c}$$

Reviews:

- F. Prino and R. Rapp, JPG(2019)
- X. Dong and V. Greco, Prog.Part.Nucl.Phys. (2019)
- Jiaying Zhao et al., arXiv:2005.08277

FUTURE:

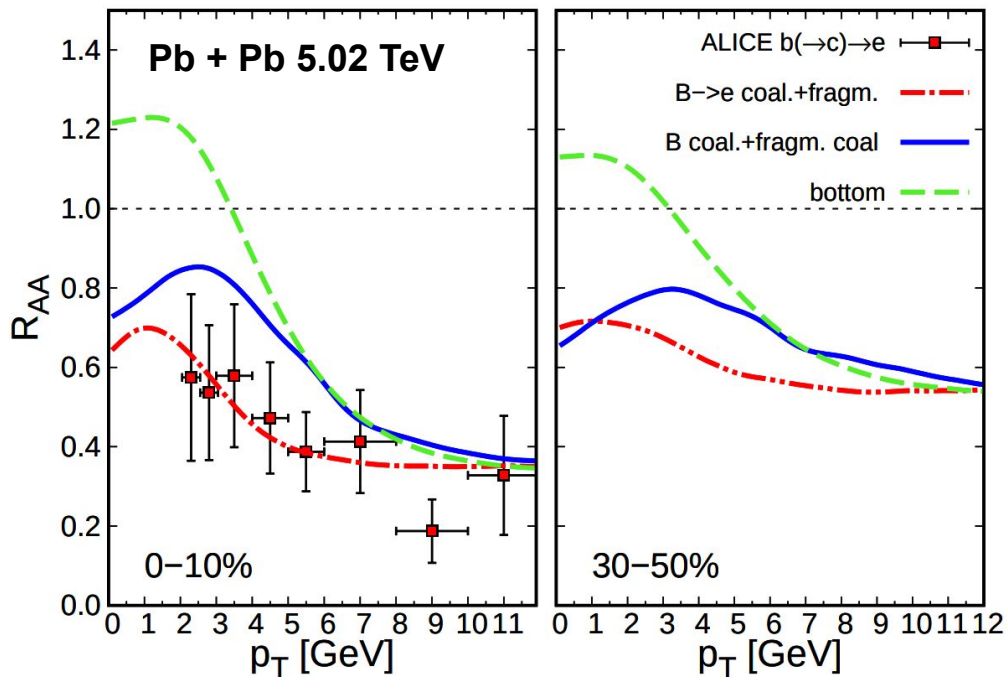
- Access low p and precision data (detector upgrade)
- Better insight into hadronization
- New observables
- Bottom** → **Main focus of this talk**

**CHARM VS BOTTOM:
D_s IN THE INFINITE MASS LIMIT**

Extension to bottom dynamics: R_{AA}

Hadronization with coalescence + fragmentation model

- Prediction for B meson R_{AA}
- R_{AA} of electrons from semileptonic B meson decay



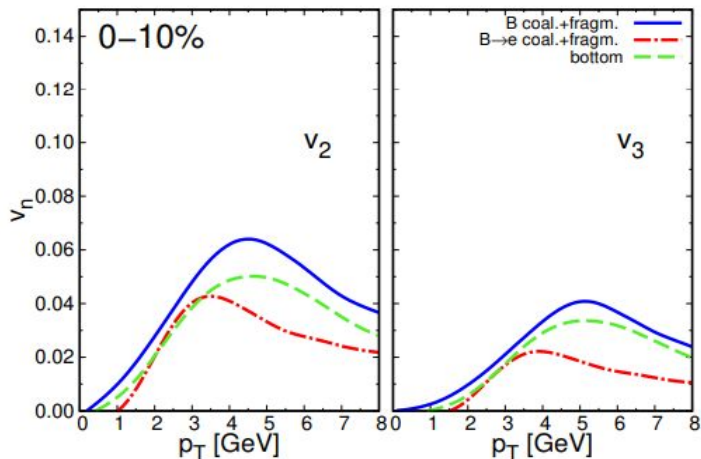
**No parameters changed
with respect to charm
dynamics \rightarrow same
interaction**

- Shift of the peak to higher momenta
➤ smaller with respect to the one
for D mesons in the same model.

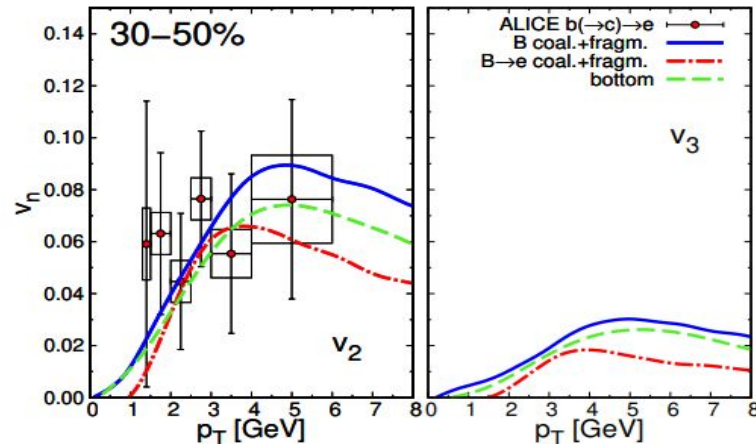
Data from: ALICE coll., arxiv:2211.13985

Extension to bottom dynamics: $v_{(n=2,3)}$ Data from ALICE, PRL 126, 162001 (2021)

- Prediction for B meson
- electrons from semileptonic B meson decay within a coal + fragm model



**No parameters changed
with respect to charm dynamics**



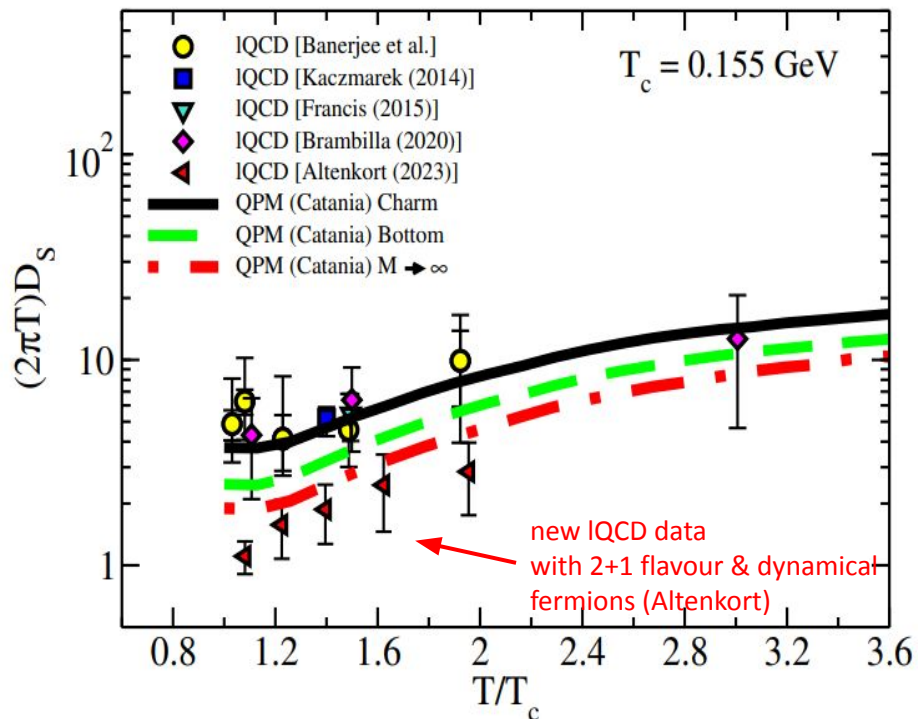
Compared to charm quark:

- Efficiency of conversion of ε_2 :
 - 15% smaller for v_2 in most central collisions.
 - 40% smaller for v_2 at 30-50% centrality.
- Efficiency of conversion of ε_3 :
 - 30% smaller for v_3 at both 0-10% and 30-50% centralities.

From central to peripheral:

- enhancement of v_2 ($\varepsilon_2(0-10\%) \approx 0.13$ and $\varepsilon_2(30-50\%) \approx 0.42$).
- Similar v_3 ($\varepsilon_3(0-10\%) \approx 0.11$ and $\varepsilon_3(30-50\%) \approx 0.21$).

$(2\pi T)D_s$: Charm quark vs Bottom quark



From D_s we obtain (in the $1-2T_c$ range):

- $\tau_{th}(c) \sim 5 \text{ fm/c}$
- $\tau_{th}(b) \sim 11 \text{ fm/c}$ breaking w.r.t. the relation:
 $\tau_{th}(b) = (M_b/M_c)\tau_{th}(c) \sim 3.3 \tau_{th}(c) \sim 16.5 \text{ fm/c}$

- IQCD data are in $M_Q \rightarrow \infty$, so the D_s evaluated is mass independent + quenched medium
- QPM use finite mass and includes dynamical fermions

$$D_s = \frac{T}{M \gamma} = \frac{T}{M} \tau_{th}$$

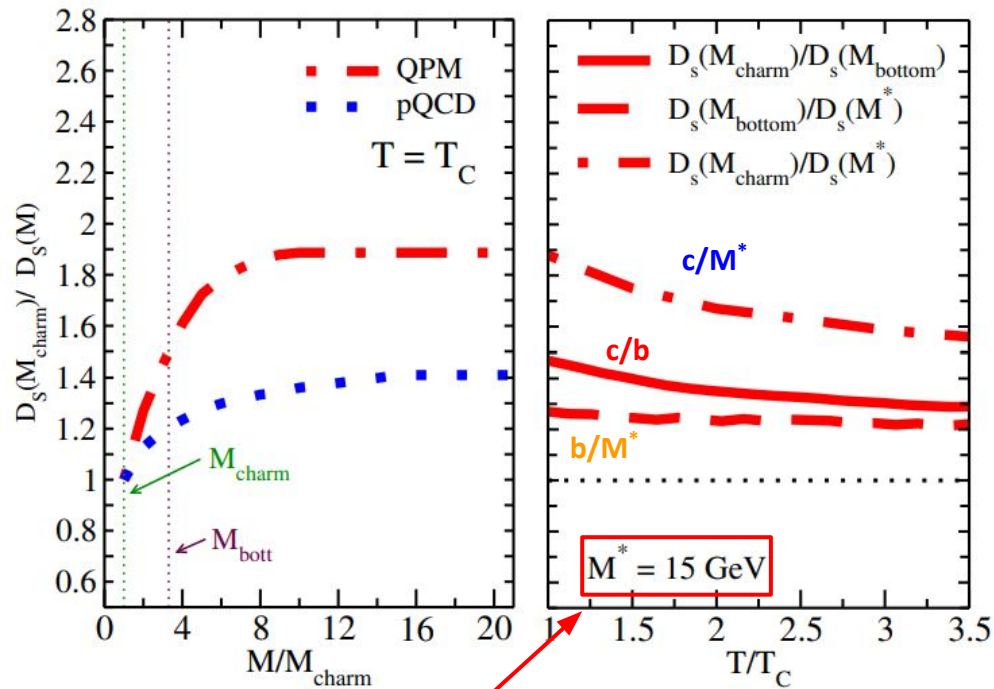
From kinetic theory is expected that:

$$\tau_{th}(b) / \tau_{th}(c) \approx \gamma_c / \gamma_b \approx M_b / M_c$$

In QPM approach $\rightarrow D_s(c)$ is 30-40% larger than $D_s(b)$ (no mass independence)

$M \rightarrow \infty$ limit is not reached for charm

$(2\pi T)D_s$ ratios: Charm quark vs Bottom quark



➤ $D_s(M_{\text{charm}})/D_s(M)$ as a function of M/M_{charm} at T_C :

Saturation scale of D_s for $M_Q \sim 8 M_{\text{charm}} \gtrsim 10 \text{ GeV}$
 $D_s(M_{\text{charm}})/D_s(M \rightarrow \infty) = 1.9$ for QPM.

$D_s(M_{\text{charm}})/D_s(M \rightarrow \infty) \approx 1.4$ for pQCD.

➤ Ratios at fixed mass as a function of T :

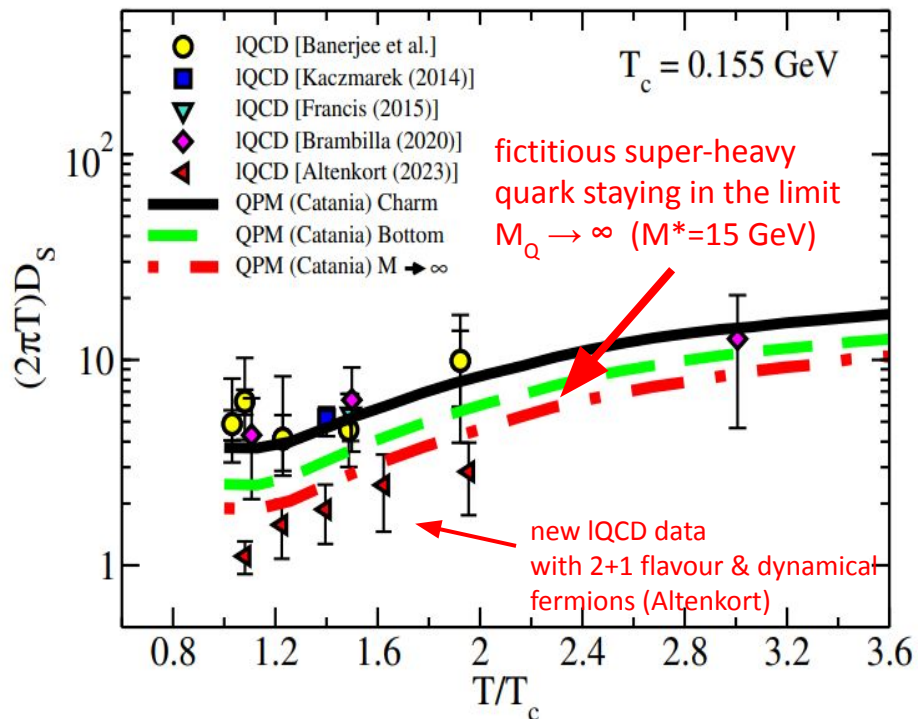
- b/M^* : about 25% in all T range

- c/b : about 50% at T_C and not smaller than 30%

- c/M^* : factor 1.5-2

fictitious super-heavy quark staying in the $M_Q \rightarrow \infty$ limit

$(2\pi T)D_s$: Charm quark vs Bottom quark



From D_s we obtain (in the $1-2T_c$ range):

- $\tau_{th}(c) \sim 5 \text{ fm}/c$
- $\tau_{th}(b) \sim 11 \text{ fm}/c$ breaking w.r.t. the relation:
 $\tau_{th}(b) = (M_b/M_c)\tau_{th}(c) \sim 3.3 \tau_{th}(c) \sim 16.5 \text{ fm}/c$

- IQCD data are in $M_Q \rightarrow \infty$ so D_s is mass independent

$$D_s = \frac{T}{M \gamma} = \frac{T}{M} \tau_{th}$$

- QPM use finite mass and includes dynamical fermions

From kinetic theory is expected that:

$$\tau_{th}(b)/\tau_{th}(c) \approx \gamma_c/\gamma_b \approx M_b/M_c$$

$D_s(T)$ from QPM in the infinite mass limit is the more pertinent to compare to IQCD simulations evaluated taking into account dynamical fermions

PRELIMINARY:

MOMENTUM DEPENDENT QPM

Going back to Quasi Particle Model (QPM)...

Equation of State and Susceptibilities

Non perturbative dynamics → M scattering matrices (q,g → Q)
evaluated by Quasi-Particle Model fit to **IQCD thermodynamics**

$N_f=2+1$
Bulk:
u,d,s

QPM Standard

$$m_g^2(T) = \frac{2N_c}{N_c^2 - 1} g^2(T) T^2$$

$$m_q^2(T) = \frac{1}{N_c} g^2(T) T^2$$

→ **Thermal masses of gluons and light quarks**

no momentum dependence

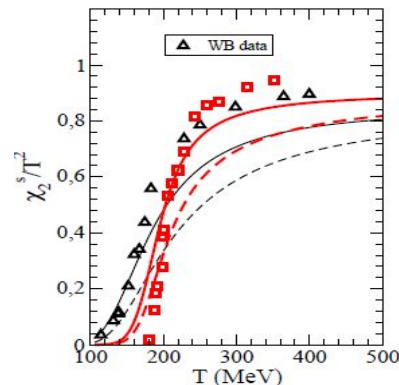
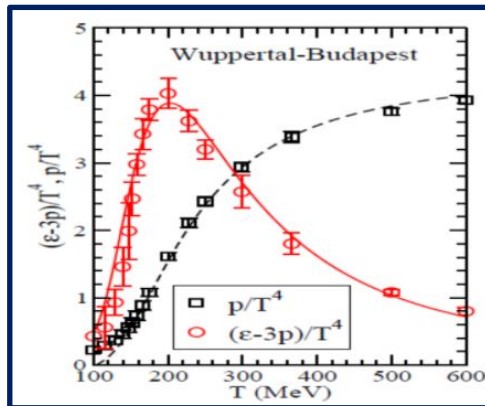
$g(T)$ from a fit to ϵ from IQCD data → good reproduction of P, $\epsilon-3P$

$$g^2(T) = \frac{48\pi^2}{(11N_c - 2N_f) \ln \left[\lambda \left(\frac{T}{T_c} - \frac{T_s}{T_c} \right) \right]^2}$$

$\lambda=2.6$
 $T_s=0.57 T_c$

Larger than pQCD especially as $T \rightarrow T_c$

Standard QPM underestimates the **quark susceptibilities**



QPM extended – momentum dependence

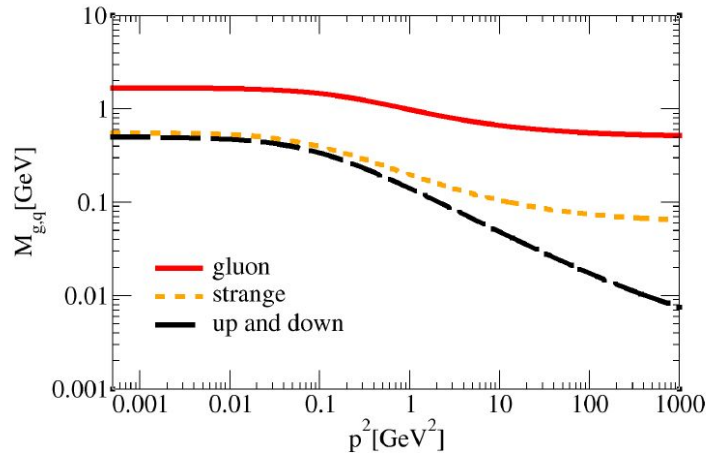
Dyson-Schwinger studies in the vacuum → following the model developed by PHSD group

H. Berrehrah, W. et al., Phys.Rev.C 93, 044914 (2016).
C. S. Fischer, J. Phys. G 32, R253 (2006).

$$M_g(T, \mu_q, p) = \left(\frac{3}{2}\right) \left(\frac{g^2(T^*/T_c(\mu_q))}{6} \left[\left(N_c + \frac{1}{2} N_f \right) T^2 + \frac{N_c}{2} \sum_q \frac{\mu_q^2}{\pi^2} \right] \left[\frac{1}{1 + \Lambda_g(T_c(\mu_q)/T^*) p^2} \right] \right)^{1/2} + m_{\chi_g}$$

$$M_{q,\bar{q}}(T, \mu_q, p) = \left(\frac{N_c^2 - 1}{8N_c} g^2(T^*/T_c(\mu_q)) \left[T^2 + \frac{\mu_q^2}{\pi^2} \right] \left[\frac{1}{1 + \Lambda_q(T_c(\mu_q)/T^*) p^2} \right] \right)^{1/2} + m_{\chi_q}$$

Momentum dependent factors



we have also extended our quasi-particle model approach for **Nf = 2+1** to **Nf = 2 + 1 + 1** where the **charm quark is included**

QPM extended – momentum dependence

Dyson-Schwinger studies in the vacuum → following the model developed by PHSD group

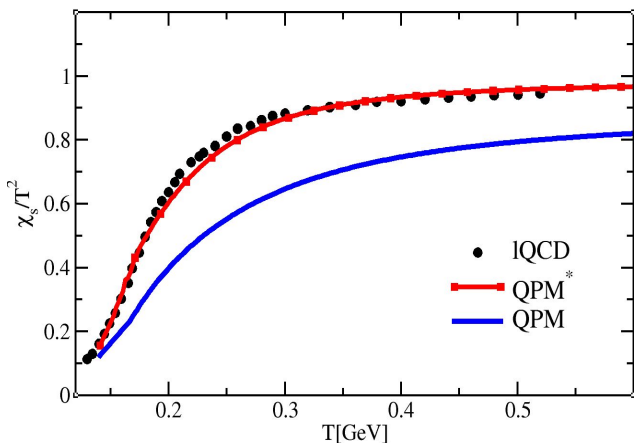
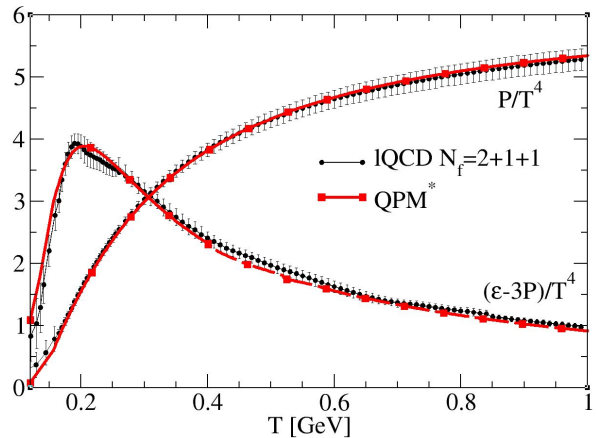
H. Berrehrah, W. et al., Phys.Rev.C 93, 044914 (2016).
C. S. Fischer, J. Phys. G 32, R253 (2006).

$$M_g(T, \mu_q, p) = \left(\frac{3}{2}\right) \left(\frac{g^2(T^*/T_c(\mu_q))}{6} \left[\left(N_c + \frac{1}{2} N_f \right) T^2 + \frac{N_c}{2} \sum_q \frac{\mu_q^2}{\pi^2} \left[\frac{1}{1 + \Lambda_g(T_c(\mu_q)/T^*) p^2} \right] \right] \right)^{1/2} + m_{\chi_8}$$

$$M_{q,\bar{q}}(T, \mu_q, p) = \left(\frac{N_c^2 - 1}{8N_c} g^2(T^*/T_c(\mu_q)) \left[T^2 + \frac{\mu_q^2}{\pi^2} \left[\frac{1}{1 + \Lambda_q(T_c(\mu_q)/T^*) p^2} \right] \right] \right)^{1/2} + m_{\chi_4}$$

Momentum dependent factors

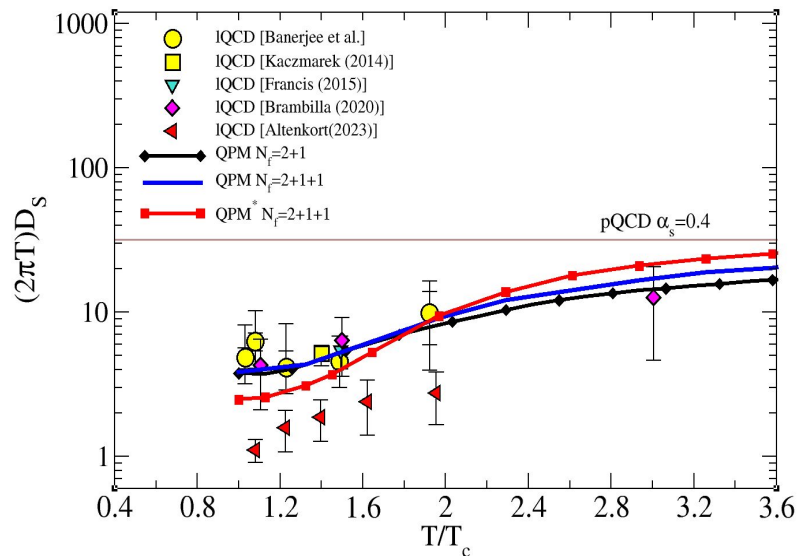
We correctly reproduce both **EoS** and **quark susceptibilities** which are underestimated in the standard QPM approach.



$$\chi_s = \frac{T}{V} \frac{\partial^2 \ln Z}{\partial \mu_s^2}$$

QUARK SUSCEPTIBILITIES

QPM extended – Preliminary D_S and R_{AA}

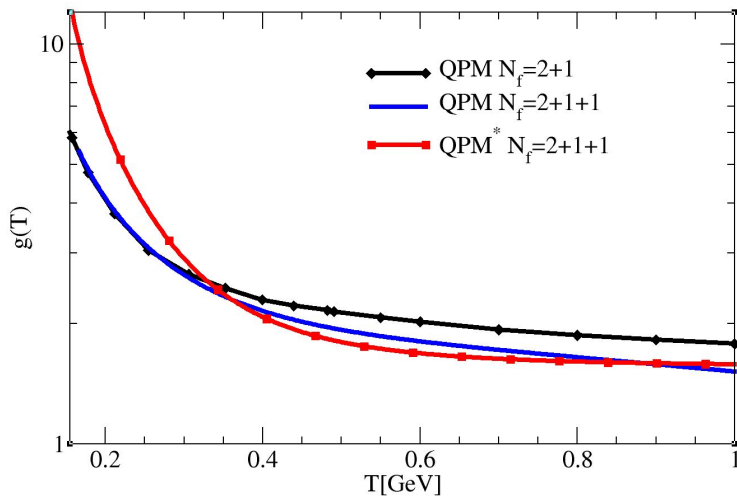


coupling $g(T)$

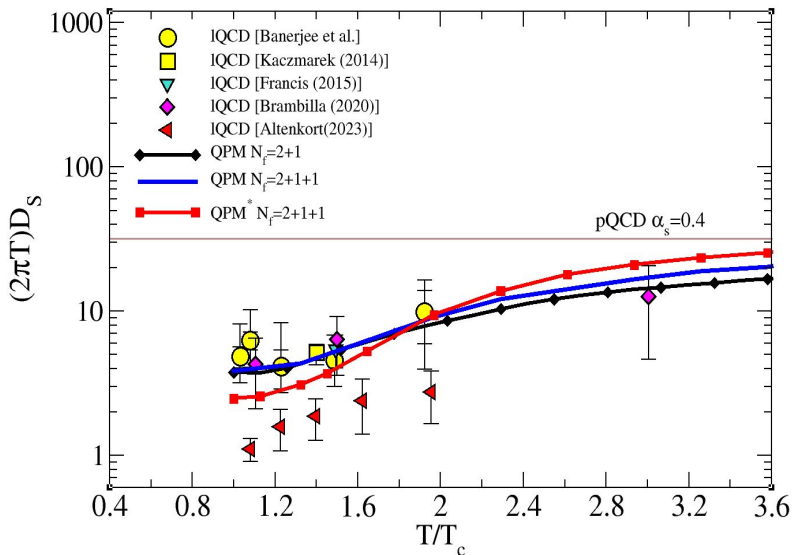
Spatial diffusion coefficient $D_S \rightarrow$ standard QPM
 standard QPM including charm
 extended QPM

$T/T_c < 2 \rightarrow$ strong non-perturbative behaviour near to T_c .

high T region \rightarrow the D_S reaches the pQCD limit quickly than the standard QPM.



QPM extended – Preliminary D_S and R_{AA}



Extended QPM + infinite mass limit?

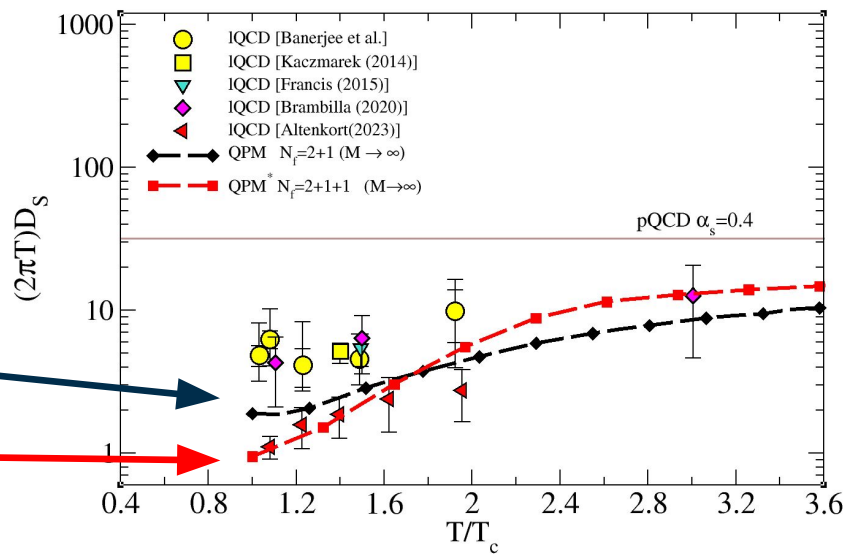
standard QPM

extended QPM

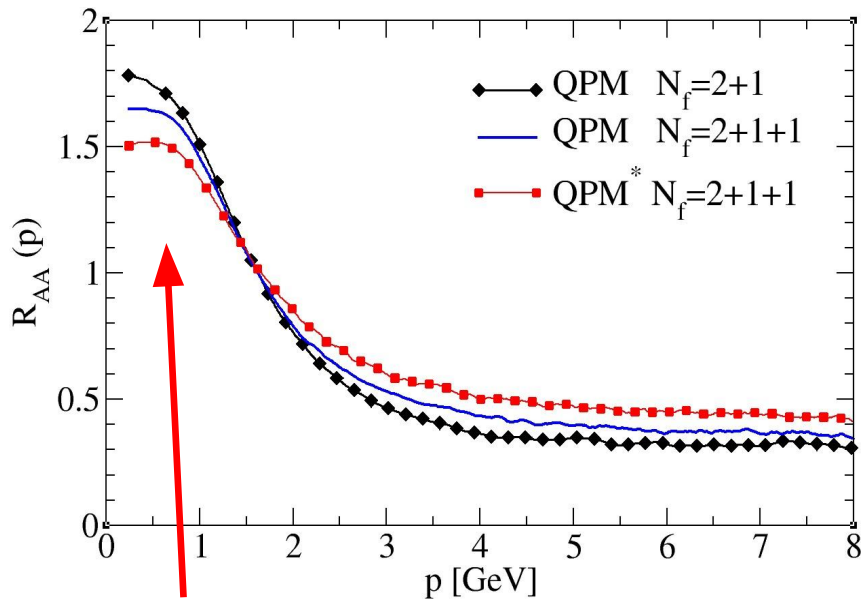
Spatial diffusion coefficient $D_S \rightarrow$ standard QPM
 standard QPM including charm
 extended QPM

$T/T_c < 2 \rightarrow$ strong non-perturbative behaviour near to T_c .

high T region \rightarrow the D_S reaches the pQCD limit quickly than the standard QPM.



QPM extended – Preliminary D_S and R_{AA}



In a static box

Initial momentum distribution function
→ FONLL for charm quark

$$R_{AA} \hat{=} f_C(p, t_f) / f_C(p, t_0)$$

Momentum dependent QPM approach

- Better description of recent IQCD data.
- Effects on the global χ^2 coming from the comparison to the experimental data of R_{AA}, v_n ?

Conclusions

- Extension to bottom quark dynamics: good description of R_{AA} and v_2 of electrons from semileptonic B meson decay and prediction for v_3
- **Spatial diffusion coefficient $D_s(T)$: charm vs bottom and the infinite mass limit**
 - $D_s(c)/D_s(b)$ ratio of about a factor of 1.5 at $T \sim T_c$ and 1.3 at higher temperatures ($T \sim 3 - 4 T_c$)
 - For the **charm mass scale**: the infinite mass limit used in IQCD is not yet reached;
For the **bottom mass scale**: discrepancy of only about a 20% w.r.t. the infinite mass limit
 - Taking into account mass scale dependence in QPM, we have satisfactory agreement with the most recent IQCD calculations that include dynamical fermions, differently from previous IQCD data in quenched approximation.
 - Thermalization time for bottom quark: $\tau_{th} \sim 10 - 12$ fm/c which is about a factor of 2 larger than charm and so quite smaller than 3.3 as suggest by a simple M_Q/T scaling.
- **Extended QPM**

Good reproduction of both EoS and susceptibilities.

Preliminary for a static medium: decrease of D_s at small T and decrease of R_{AA} at low p

Perspectives: Effect on observables for realistic simulations?

Thanks for the attention!

Back up slides

Relativistic Boltzmann equation at finite η/s

Bulk evolution

$$p^\mu \partial_\mu f_q(x, p) + m(x) \partial_\mu^x m(x) \partial_p^\mu f_q(x, p) = C[f_q, f_g]$$

$$p^\mu \partial_\mu f_g(x, p) + m(x) \partial_\mu^x m(x) \partial_p^\mu f_g(x, p) = C[f_q, f_g]$$

Free-streaming

field interaction

$$\varepsilon - 3p \neq 0$$

HQ evolution

$$p^\mu \partial_\mu f_Q(x, p) = C[f_q, f_g, f_Q]$$

$$C[f_q, f_g, f_Q] = \frac{1}{2E_1} \int \frac{d^3 p_2}{2E_2 (2\pi)^3} \int \frac{d^3 p_1'}{2E_1' (2\pi)^3}$$

$$\times [f_Q(p_1') f_{q,g}(p_2') - f_Q(p_1) f_{q,g}(p_2)]$$

$$\times |M_{(q,g) \rightarrow Q}(p_1 p_2 \rightarrow p_1' p_2')|$$

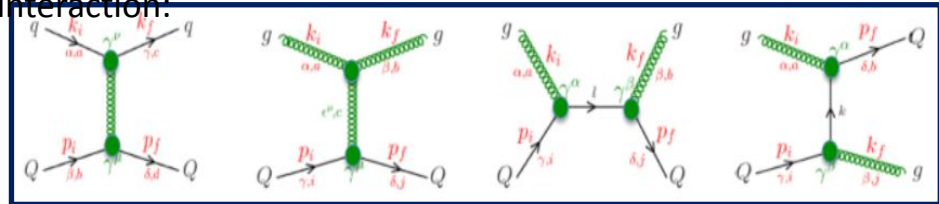
$$\times (2\pi)^4 \delta^4(p_1 + p_2 - p_1' - p_2')$$

Collision Integral gauged to reproduce viscous Hydro at fixed η/s by means of Chapman-Enskog

$$\sigma(n(\vec{x}), T) = \frac{1}{15} \frac{\langle p \rangle_0}{g(a)n(\vec{x})} \frac{1}{\eta/s}$$

Equivalent to viscous hydro at $\eta/s \approx 0.1$

Feynmann diagrams at first order pQCD for HQs-bulk interaction:

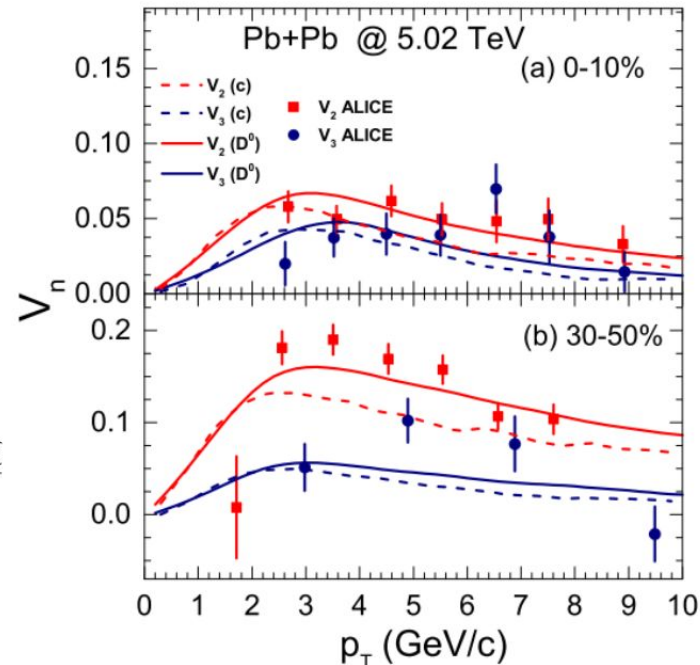
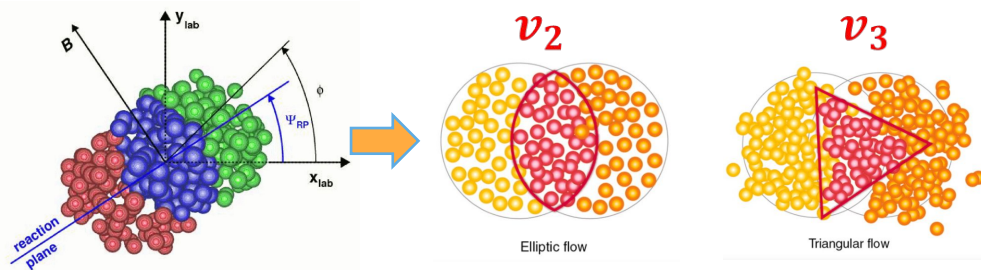


Scattering matrices $M_{g,q}$ by QPM fit to IQCD thermodynamics

Extension to higher order anisotropic flows $v_n(p_T)$

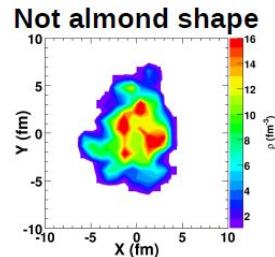
$$E \frac{d^3N}{dp_T} = \frac{1}{2\pi} \frac{d^2N}{p_T d\phi dy} \left\{ 1 + \sum_{n=1}^{\infty} v_n \cos[n(\phi - \Psi_n)] \right\}$$

Sambataro et al., *Eur.Phys.J.C* 82 (2022) 9, 833



Monte Carlo Glauber for initial condition of partons

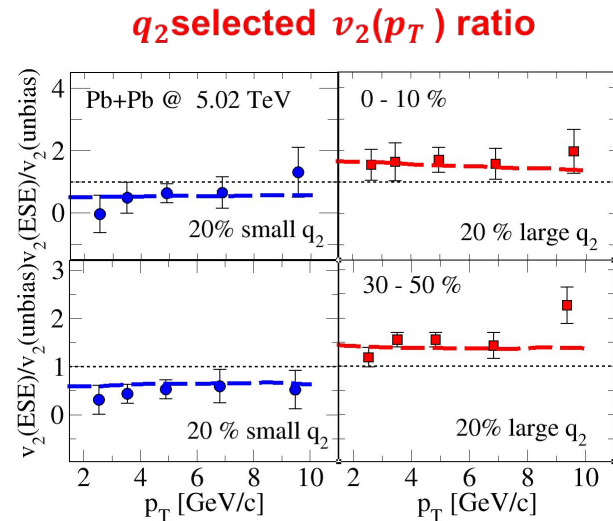
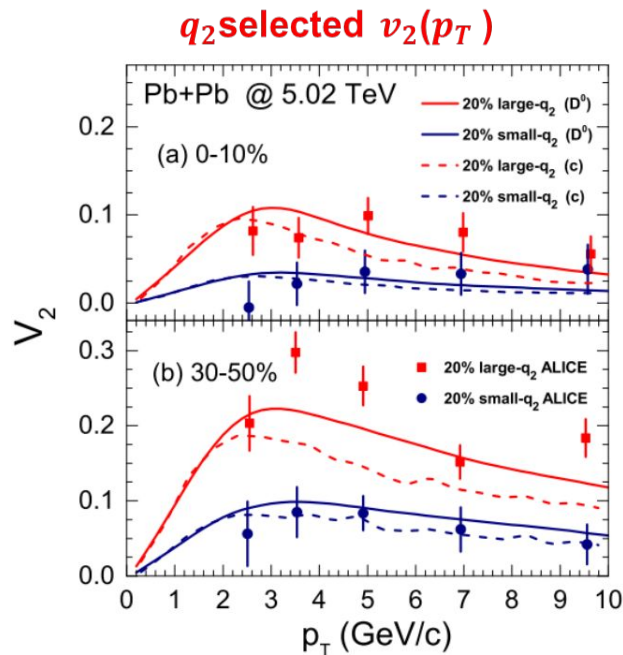
S.Plumari et al, *Phys.Rev.C* 92 (2015) 5



Data taken from ALICE collaboration: *Phys.Lett.B* 813 (2021) 136054

- In the more peripheral collision (30-50 % centrality class) \rightarrow larger v_2 and comparable v_3
- \triangleright v_2 mainly generated by the geometry of overlapping region in larger centrality collision
 - \triangleright v_3 mainly driven by the fluctuation of the triangularity of overlap region at all centrality

ESE: v_2 and spectra (20% small/large q_2)



Data taken from ALICE collaboration:
Phys.Lett.B 813 (2021) 136054

➤ v_2 (large- q_2 /small- q_2) $\cong v_2$ (unbiased) of **about 50%** in both 0-10% and 30-50% centrality.

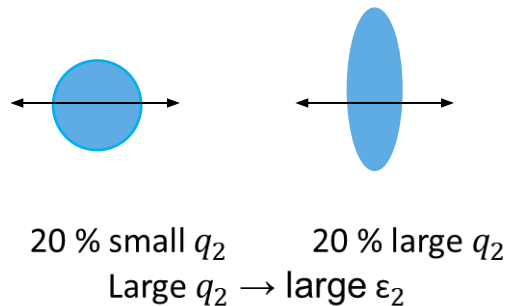
Extension to higher order anisotropic flows $v_n(p_T)$

ESE technique and v_n correlations

Selection of events with the **same centrality** but **different initial geometry** on the basis of the magnitude of the second-order harmonic reduced flow vector q_2 .

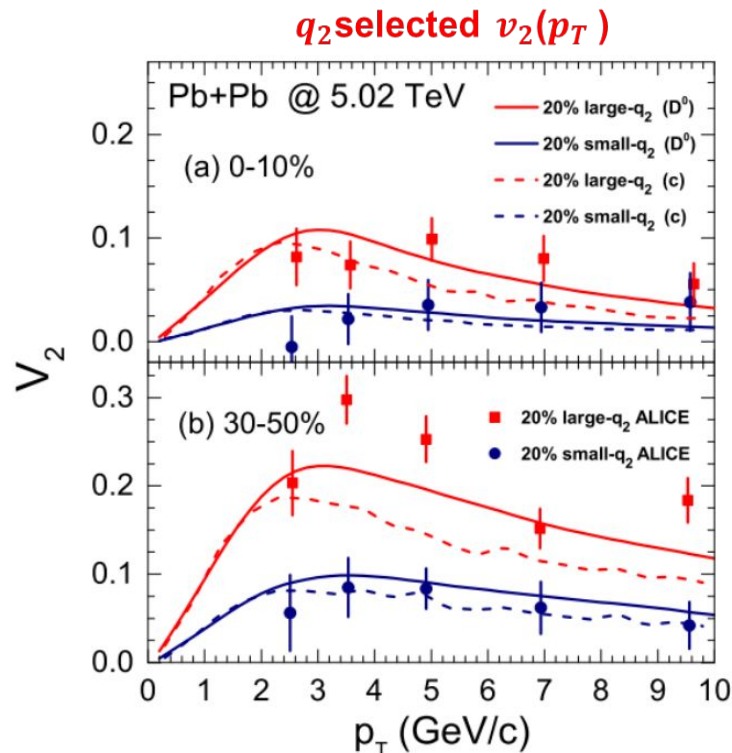
$$q_2 = |\vec{Q}_2|/\sqrt{M}$$

$$\vec{Q}_2 = \sum_{j=1}^M e^{i2\varphi_j}$$



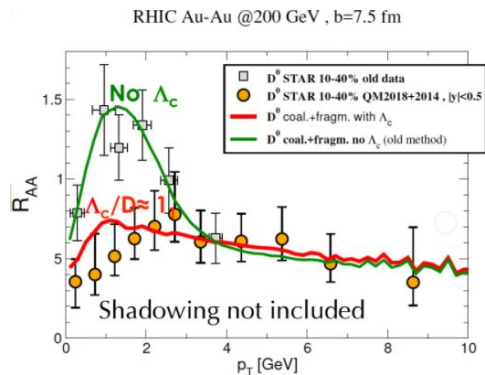
$$\epsilon_n = \frac{\langle r_\perp^n \cos[n(\varphi - \Phi_n)] \rangle}{\langle r_\perp^n \rangle} \quad \Phi_n = \frac{1}{n} \arctan \frac{\langle r_\perp^n \sin(n\varphi) \rangle}{\langle r_\perp^n \cos(n\varphi) \rangle}$$

$$r_\perp = \sqrt{x^2 + y^2}, \quad \varphi = \arctan(y/x)$$

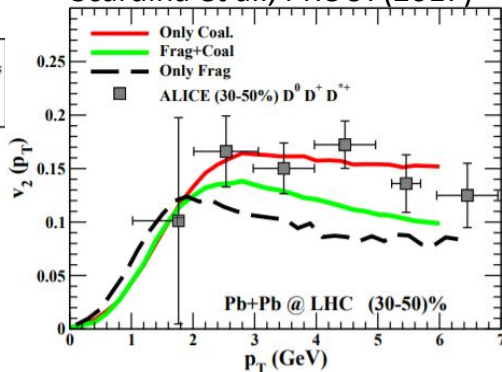


Data from ALICE collaboration:
Phys.Lett.B 813 (2021) 136054

Catania QPM: some prediction for charm...



Scardina et al., PRC 97(2017)



Good description of

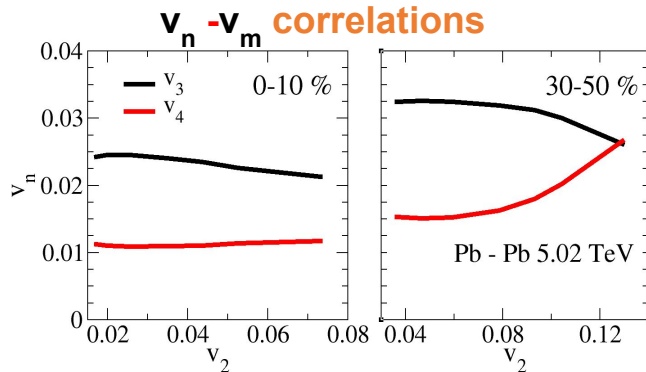
R_{AA}, v_2 at RHIC & LHC energies
within error bars

Monte Carlo Glauber for initial
condition of partons

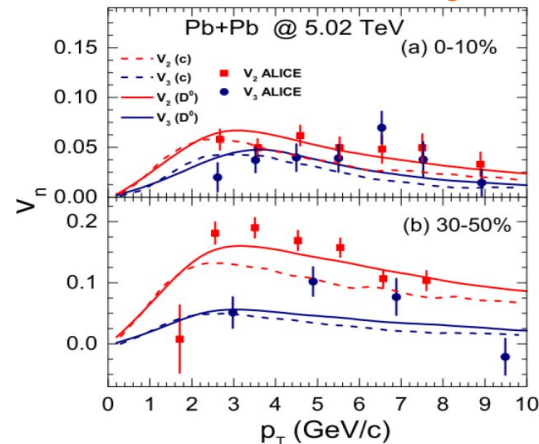
S.Plumari et al, *Phys.Rev.C* 92 (2015) 5

Predictions for D mesons

- Event-Shape Engineering Technique: Prediction for similar correlation for hard particles wrt bulk



Triangular flow v_3



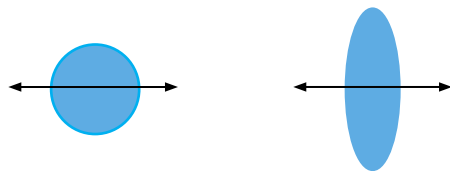
Extension to higher order anisotropic flows $v_n(p_T)$

ESE technique and v_n correlations

Selection of events with the **same centrality** but **different initial geometry** on the basis of the magnitude of the second-order harmonic reduced flow vector q_2 .

$$q_2 = |\vec{Q}_2| / \sqrt{M}$$

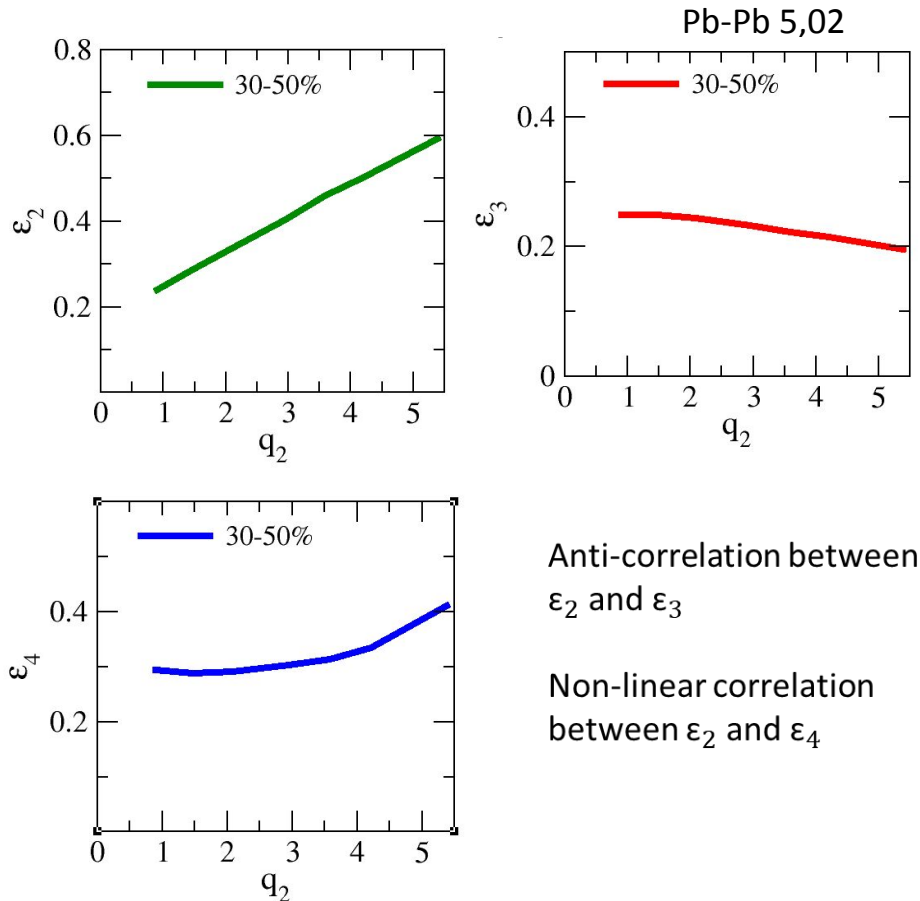
$$\vec{Q}_2 = \sum_{j=1}^M e^{i2\varphi_j}$$



20 % small q_2 20 % large q_2
 Large $q_2 \rightarrow$ large ϵ_2

Monte Carlo Glauber for initial condition of partons

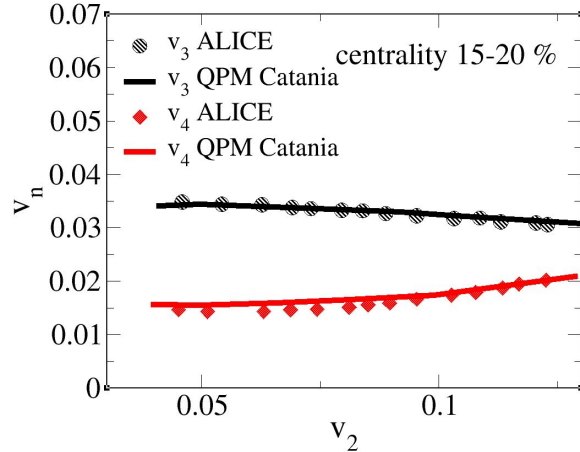
S.Plumari et al, *Phys.Rev.C* 92 (2015) 5



ESE: $v_n - v_m$ correlations

M.L. Sambaturo, et al., *Eur.Phys.J.C* 82 (2022)

Charged particles

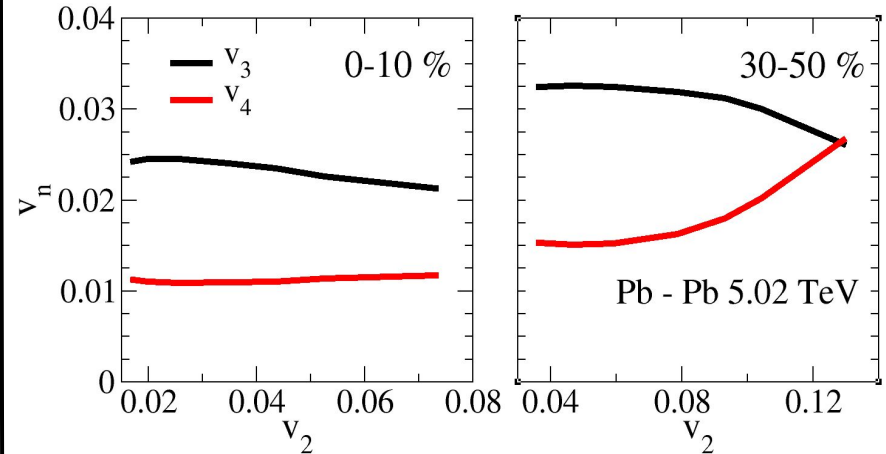


Correlations between the ϵ_n and ϵ_m present in the initial geometry \rightarrow correlations between flow harmonics different orders, i.e. correlations v_n and v_m

- Good description of v_{n-m} correlation for bulk
- Prediction for similar correlation for hard particles
- Correlation for D mesons provide insights on the interaction

Plumari et al, *Phys.Lett.B* 805 (2020) 135460

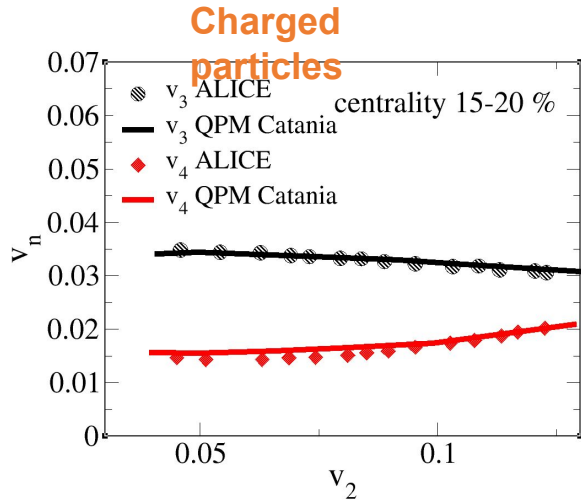
Predictions for D mesons



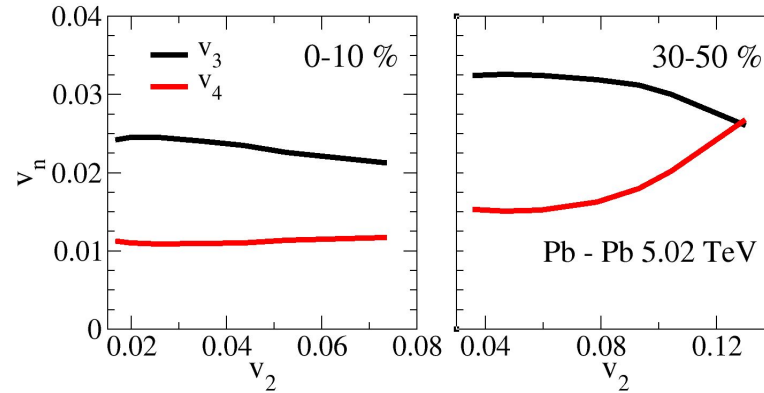
Data taken from: S. Mohapatra *Nucl.Phys.A* 956 (2016) 59-66

ESE: $v_n - v_m$ correlations

M.L. Sambataro, et al., *Eur.Phys.J.C* 82 (2022)



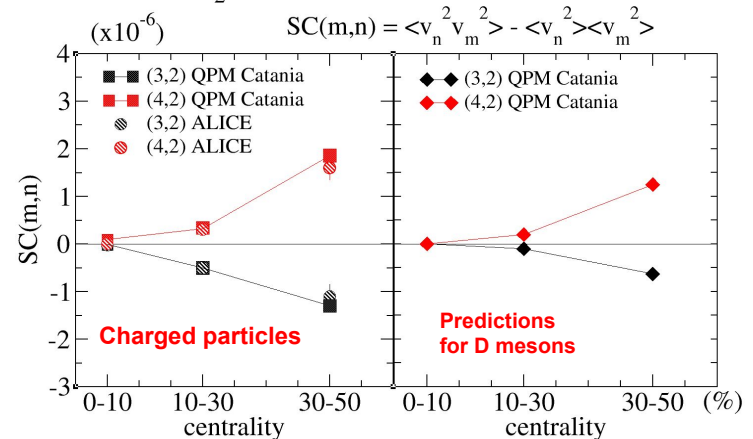
Predictions for D



Correlations between the ϵ_n and ϵ_m present in the initial geometry \rightarrow correlations between flow harmonics different orders, i.e. correlations v_n and v_m

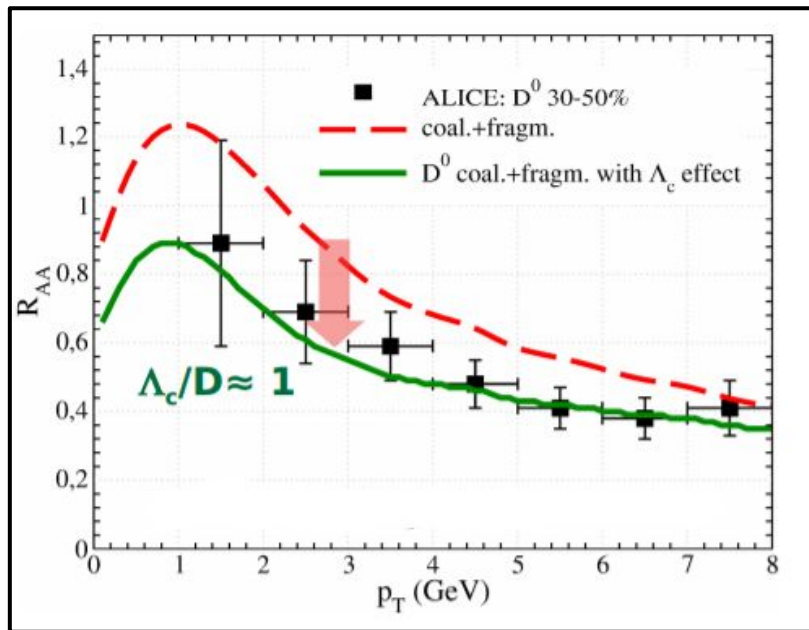
- Good description of v_{n-m} correlation for bulk particles
- Prediction for similar correlation for hard particles
- Correlation for D mesons provide insights on the interaction and its temperature dependence

Plumari et al, *Phys.Lett.B* 805 (2020) 135460



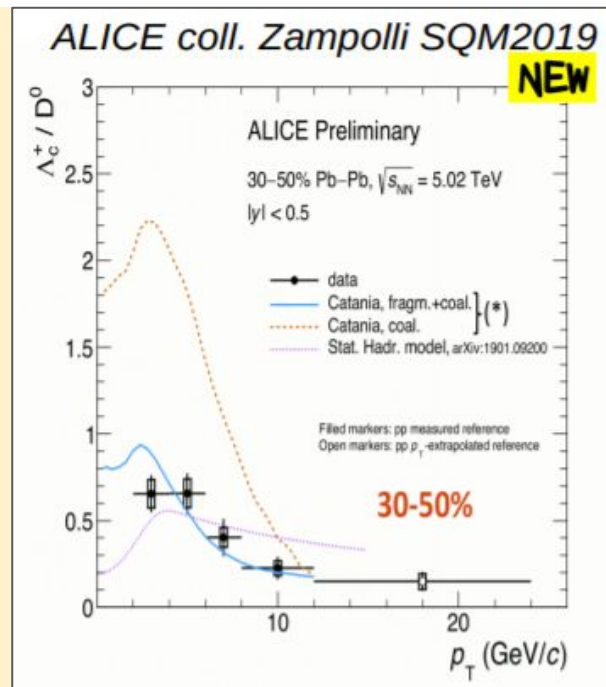
Data taken from: S. Mohapatra *Nucl.Phys.A* 956 (2016) 59-66

D meson: Impact of large Λ_c production on R_{AA}



$D_s(T)$ of charm quark that reproduces R_{AA} and v_2 gives good description of

- Impact of Λ_c/D^0
- Triangular flow $v_3(p_T)$.
- q_2 selected anisotropic flow and spectra.



- With the same coalescence plus fragmentation model we describe the Λ_c/D^0

S. Plumari, et al.,
Eur. Phys. J. C78 no. 4, (2018) 348

Numerical solution of Boltzmann Equation

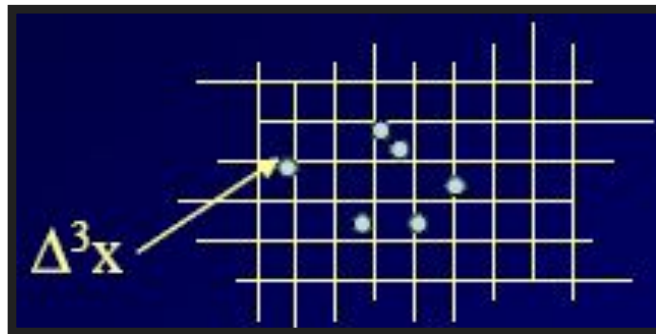
- Use Test-Particle Method to sample the phase space distribution function

$$f(\vec{x}, \vec{p}, t) = \omega \sum_{i=1}^{N_{test}} \delta^{(3)}(\vec{x} - \vec{r}_i(t)) \delta^{(3)}(\vec{p} - \vec{p}_i(t))$$

F_i solution of Boltzmann eq.

→ Test particles solve classical Hamilton eq. of motion

$$\begin{cases} \vec{p}_i(t + \Delta t) = \vec{p}_i(t - \Delta t) + 2\Delta t \cdot \left(\frac{\partial \vec{p}_i}{\partial t} \right)_{coll} \\ \vec{r}_i(t + \Delta t) = \vec{r}_i(t - \Delta t) - 2\Delta t \cdot \left[\frac{\vec{p}_i(t)}{E_i(t)} \right] \end{cases}$$



- Collision Integral mapped through a Stochastic Algorithm

$$P_{22} = \frac{\Delta N_{coll}^{2 \rightarrow 2}}{\Delta N_1 \Delta N_2} = v_{rel} \sigma_{22} \frac{\Delta t}{\Delta^3 x}$$

$\Delta t \ll 0$ and $\Delta^3 x \ll 0$: exact solution

Final phase-space of HQ + bulk parton scattering sampled according to $|M_{QCD}|^2$ □ code test through simulations in a “box”

[Scardina, Colonna, Plumari, and Greco PLB v.724, 296 (2013)]

[Xu and Greiner PRC v. 71, (2005)]

Hybrid Hadronization Model for HQs

✓ **COALESCENCE**: Formula developed for the light sector [Greco, Ko, Levai PRL 90 (2003)]

$$\frac{dN_H}{d^2\mathbf{P}_T} = g_H \int \prod_{i=1}^n \frac{d^3 p_i}{(2\pi)^3 E_i} p_i \cdot d\sigma_i f_{q_i}(x_i, p_i) f_W(x_1 \dots x_n; p_1 \dots p_n) \delta\left(\mathbf{P}_T - \sum_i^n p_{T,i}\right)$$

Statistical Factor
Color-spin-isospin

Parton Distribution Functions
(after Boltzmann evolution)

Hadron Wigner Function

(parameters fix according to quark model)

C.-W. Hwang, EPJ C23, 585 (2002)

C. Albertus et al., NPA 740, 333 (2004)

✓ **FRAGMENTATION**: HQs that do not undergo to Coalescence

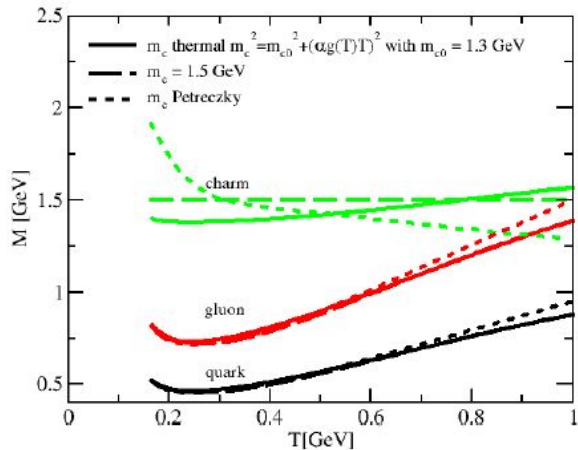
$$\frac{dN_H}{d^2\mathbf{P}_T} = \sum_f \int dz \frac{dN_f}{d^2 p_T} \frac{D_{f \rightarrow H}(z)}{z^2}$$

We use Peterson parametrization: $D_H(z) \propto \left[z \left(1 - \frac{1}{z} - \frac{\epsilon_c}{1-z} \right)^2 \right]^{-1}$ Peterson et al. PRD 27 (1983) 105

Parameter ϵ_c tuned to reproduce D and B meson spectra in pp collisions.

QPM with $N_f = 2 + 1 + 1$ including charm

Recently, new lattice results for the equation of state of QCD with 2+1+1 dynamical flavors have become available. Therefore, we extend our QPM approach for $N_f = 2 + 1$ to $N_f = 2 + 1 + 1$ where the charm quark is included.



Three cases:

Constant mass

$$m_c = 1.5 \text{ GeV}$$

Thermal mass

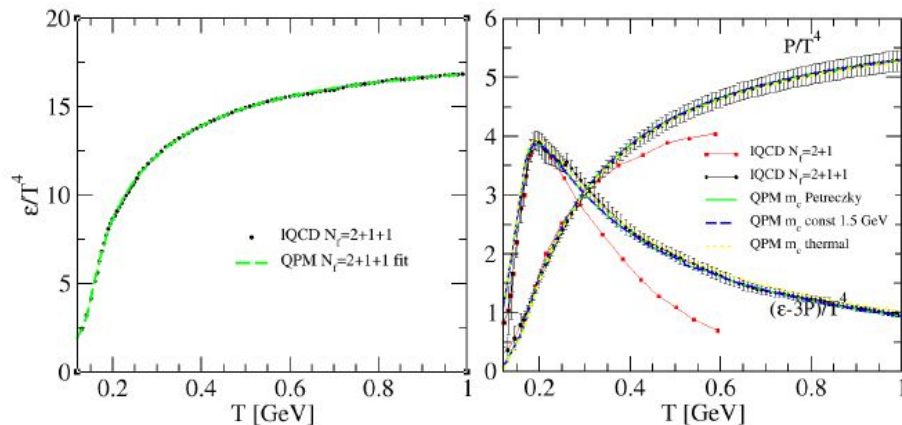
$$m_c^2 = m_{c0}^2 + \frac{N_c^2 - 1}{8N_c} g^2 T^2$$

Charm Mass constrained by quark susceptibility from IQCD

m_c [Petreczky]

□ Energy density fit to IQCD data

□ Good reproduction of **pressure** and **interaction measure** for three different charm quark masses.



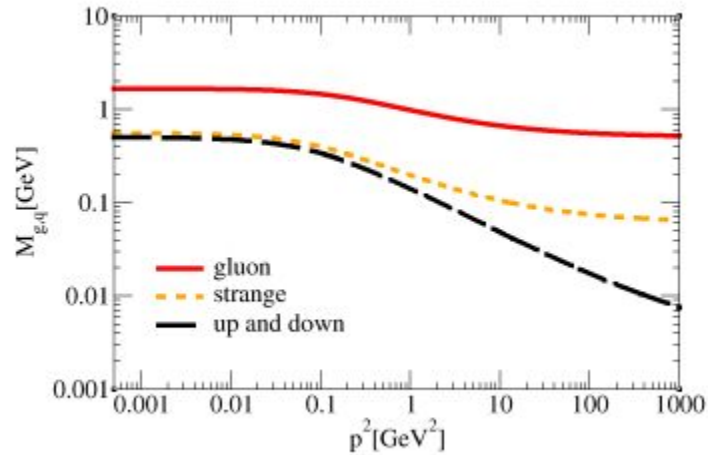
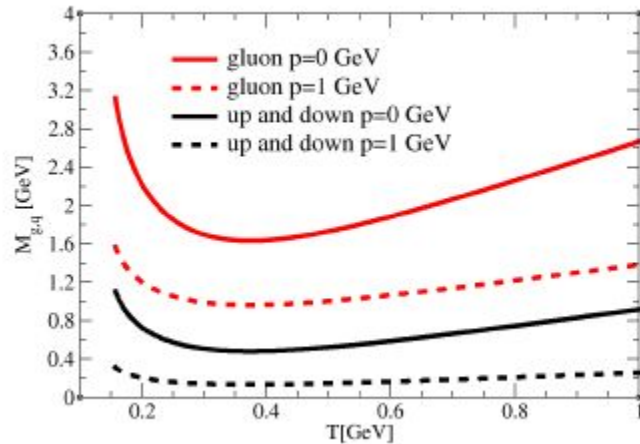
QPM extended – momentum dependence

Dyson-Schwinger studies in the vacuum → following the model developed by PHSD group

$$M_g(T, \mu_q, p) = \left(\frac{3}{2}\right) \left(\frac{g^2(T^*/T_c(\mu_q))}{6}\right) \left[\left(N_c + \frac{1}{2}N_f\right) T^2 + \frac{N_c}{2} \sum \frac{\mu_q^2}{\pi^2} \left[\frac{1}{1 + \Lambda_g(T_c(\mu_q)/T^*)p^2} \right] \right]^{1/2} + m_{\chi g}$$

$$M_{q,\bar{q}}(T, \mu_q, p) = \left(\frac{N_c^2 - 1}{8N_c}\right) g^2(T^*/T_c(\mu_q)) \left[T^2 + \frac{\mu_q^2}{\pi^2} \left[\frac{1}{1 + \Lambda_q(T_c(\mu_q)/T^*)p^2} \right] \right]^{1/2} + m_{\chi q}$$

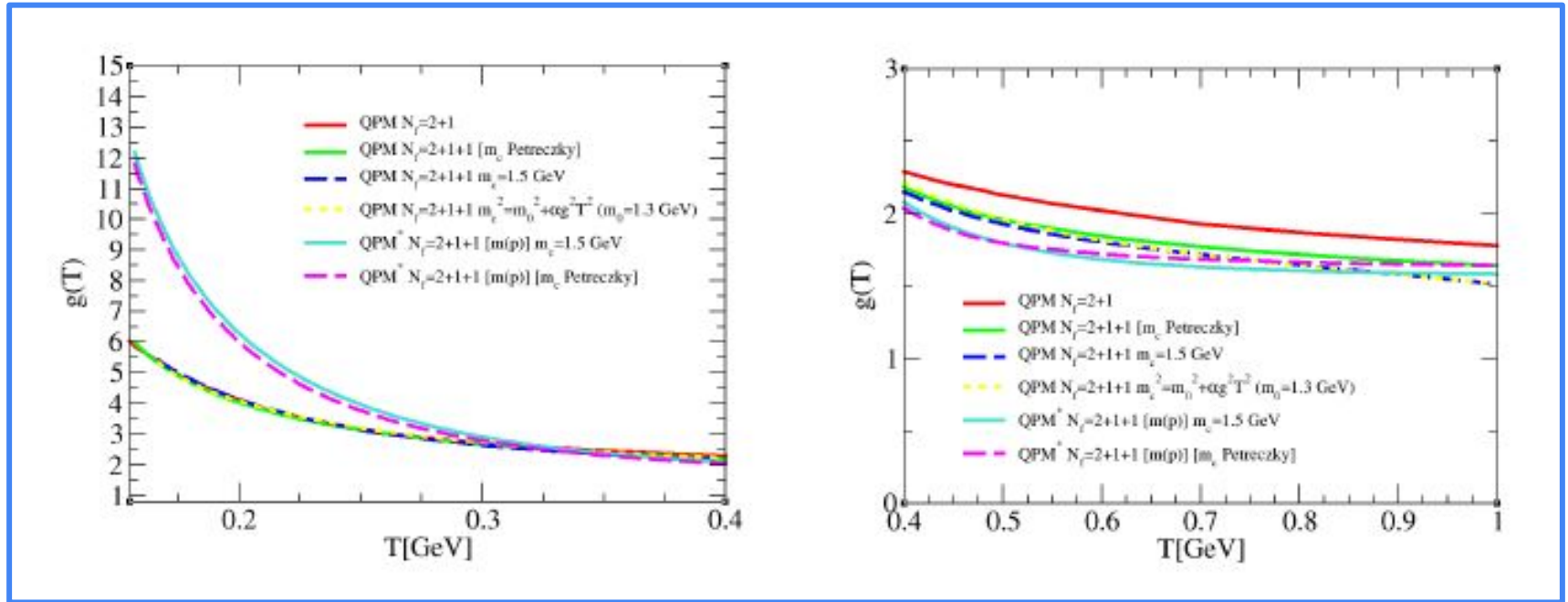
Momentum dependent factors



QPM extended – coupling and drag coefficient

$0,155 < T < 0,4 \text{ GeV}$

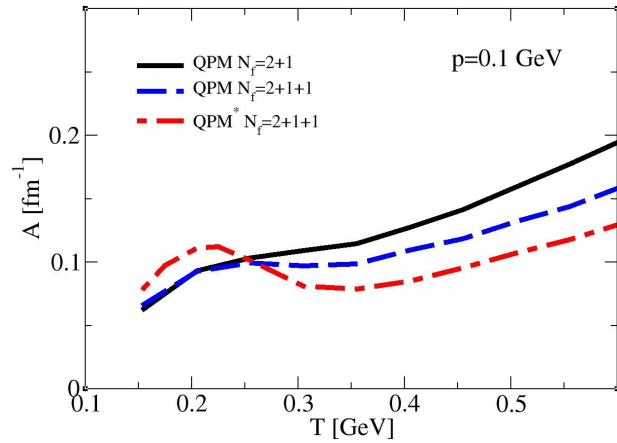
$0,4 < T < 1 \text{ GeV}$



Coupling $g(T) \rightarrow$ **standard QPM** vs **extended QPM**

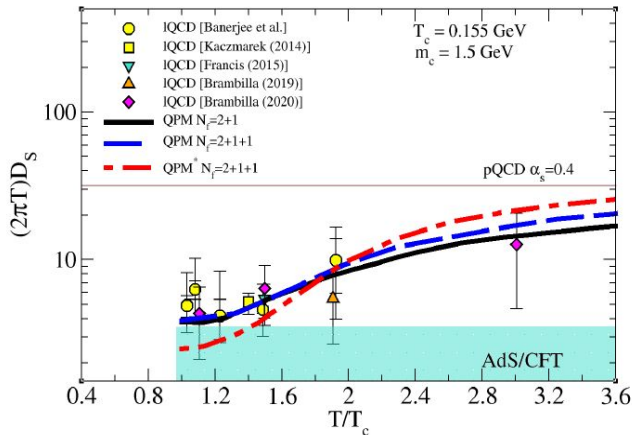
- Large enhancement at low T
- Comparable value at high T with a discrepancy

Drag and D_S in QPM extended



Drag coefficient → standard QPM
 standard QPM including charm
 extended QPM

- **Increase** at low T consistent with the large enhancement of the coupling in the same T region
- **Decrease** at high T



Spatial diffusion coefficient D_S


$T/T_c < 2 \rightarrow$ strong non-perturbative behaviour near to T_c .

high T region \rightarrow the D_S reaches the pQCD limit quickly than the standard QPM.

DQPM Dynamical Quasi-particle Model

In order to determinate the parton masses and widths within the DQPM approach, the analytical expression of the dynamical quasi-particle entropy density s_{DQP} is fitted to the IQCD entropy density s_{IQCD} determined numerically:

$$s_{DQP} = - \sum_{i=g,q,\bar{q}} \int \frac{d^3p}{2\pi (2\pi)^3} \frac{\partial n_{B/F,F}}{\partial T} \times (\mathcal{I} \ln(-\Delta_i^{-1}) + \mathcal{I} \Pi_i \mathcal{R} \Delta_i)$$



 Quasi-particle contribution interaction
 contribution

The **spectral functions** within DQPM approach describe the variation of parton masses as a function of the medium properties with result that these spectral functions are no longer δ functions in the invariant mass squared (as in the case for bare masses) but related to the imaginary part of the trace of the effective propagator $D_{\nu\mu}$ and to the partonic self-energies $\Sigma_{\nu\mu}$ as:

$$S(p) \propto \mathcal{I} D_{\mu}^{\mu}(p) \propto \frac{\mathcal{I} \Sigma_{\mu}^{\mu}(p)}{[p^2 - \mathcal{R} \Sigma_{\mu}^{\mu}(p)]^2 + [\mathcal{I} \Sigma_{\mu}^{\mu}(p)]^2}$$

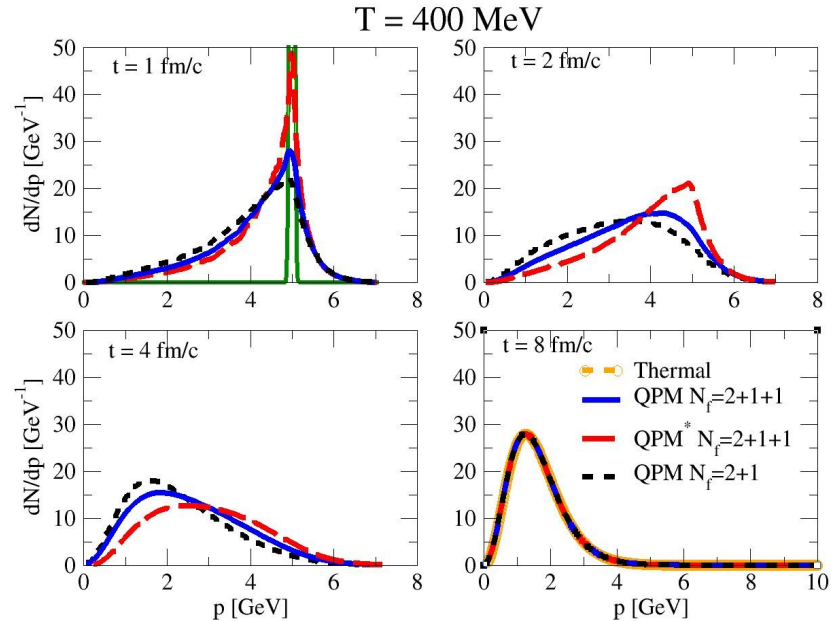
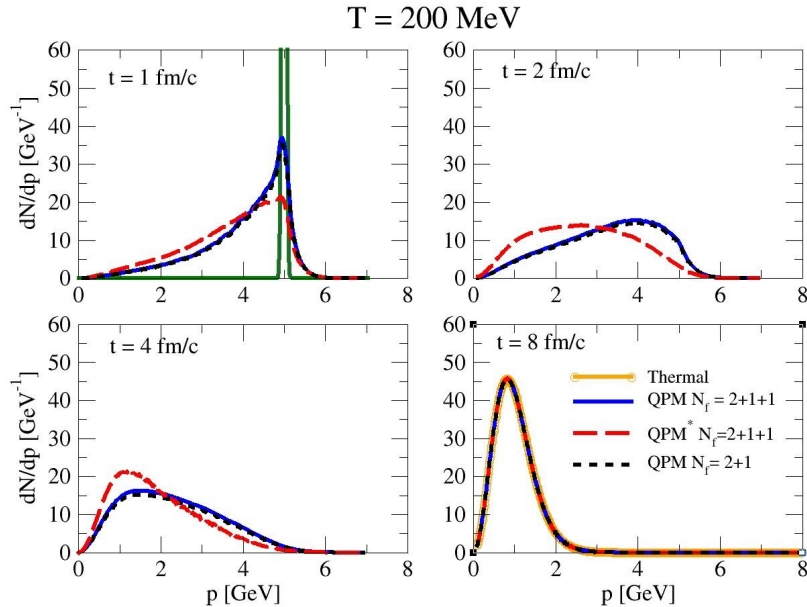
41

⌋ Self energy

Preliminary: Off-shell

BOX CALCULATION FOR CHARM \rightarrow static medium

evolution of charm quark distribution function

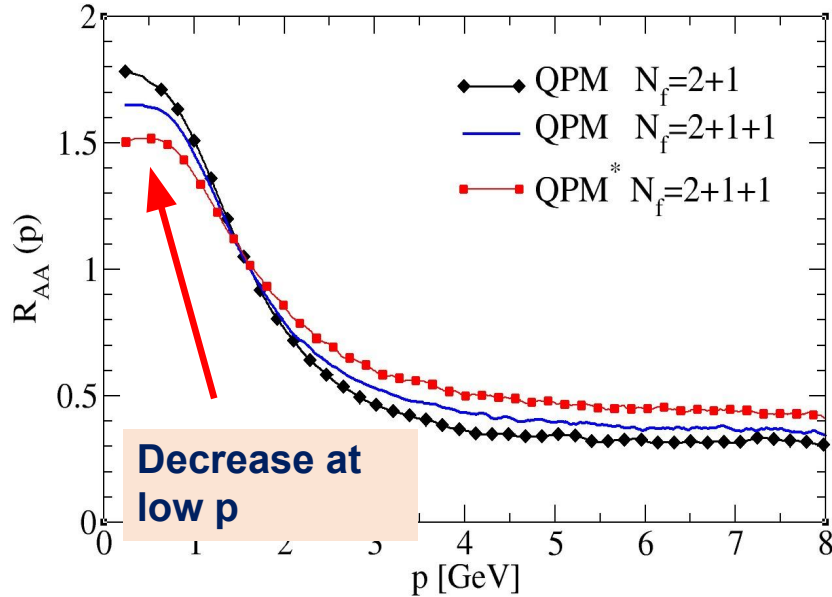


Extended QPM:

- $T > T_c$ slower dynamics
- $T \rightarrow T_c$ the increase in the drag coefficient leads to a faster evolution

Preliminary:

Nuclear modification factor R_{AA}



$$R_{AA} = \hat{f}_C(p, t_f) / f_C(p, t_0)$$

Initial momentum distribution function
 → FONLL for charm quark

Momentum dependent QPM approach

- Better description of recent IQCD data.
- Effects on the global χ^2 coming from the comparison to the experimental data of R_{AA}, v_n ?